Structure and dynamics of a monolayer KCN film grown onto a KBr(001) substrate

Jeff Baker, Jaime A. Li, and J. G. Skofronick
Department of Physics and MARTECH, Florida State University, Tallahassee, Florida 32306-4350

S. A. Safron
Department of Chemistry and MARTECH, Florida State University, Tallahassee, Florida 32306-4390
(Received 28 July 1998; revised manuscript received 1 March 1999)

Helium atom scattering was used to investigate the surface structure and dynamics of a monolayer film of KCN grown onto the nearly lattice-matched KBr(001) substrate. Although previous studies had shown that the cleaved (001) surface of KCN is disordered, the film appeared stabilized on this substrate with an ordered (001) surface. At about $T_c \approx 97$ K, the film appears to undergo a second-order phase transition from a high-temperature (1×1) phase to a low-temperature $(1\times2)/(2\times1)$ phase with an antiferroelectric alignment of the CN^- ions. For a monolayer of mixed $KBr_{0.17}(CN)_{0.83}$, this transition temperature is reduced to 78 K. In addition, for the pure KCN films, diffraction features appear for the low-temperature phase, which corresponds to a $2\sqrt{2}\times6\sqrt{2}R45°$ superstructure. Finally, measurements of the surface dispersion curves in the [100] and [110] directions provide evidence for a Rayleigh mode and a dispersionless mode at 11.5 meV, which are essentially identical above and below T_c. [S0163-1829(99)13427-1]

I. INTRODUCTION

The surface structure and phonons of the alkali halides have been studied extensively by helium atom scattering (HAS) experiments. Because one can easily prepare stable surfaces of these materials that yield superb scattering signals and because they provide suitable substrates for a wide range of materials in epitaxial growth studies, they have become model systems for helium scattering measurements and benchmark surfaces for theoretical comparisons.[1]

The KCN crystal closely resembles the alkali halide KBr (Ref. 2) in several ways, but its behavior is considerably more complex due to the vibrational (and rotational) degrees of freedom and the dipolar (and quadrupolar) interactions, which the CN^- ions add to the dynamics.[3–15] Because of this, one expects the KCN surface to exhibit a correspondingly richer behavior than that of KBr. Moreover, since KCN is miscible in KBr at all concentrations, investigations of the surfaces of the mixed crystals, $KBr_x(CN)_{1-x}$, should be as interesting and fruitful as have been those of the bulk mixed crystals.[16–23]

From its melting point at 908 K down to 168 K, bulk KCN has a face-centered-cubic lattice with the rocksalt structure,[11,22] with the CN^- confined within an octahedral cage of K^+ ions.[12] A first-order structural phase transition occurs at 168 K, taking KCN from cubic to orthorhombic, with shearing by 10.5° and contraction by about 6% of the unit cell.[10,11,22] This ferroelastic transition is accompanied by the formation of domains, which causes the crystal to change from transparent to milky white.[5] In this phase, the CN^- ions become ordered parallel to each other but retain head-to-tail disorder with respect to the CN^- electric dipoles.[10] This disorder is removed in the alternating head-to-tail antiferroelectric structure that forms at 83 K in a second-order phase transition.[6,11,22]

The cleaved (001) surface of single-crystal KCN has been investigated by this group in a number of experiments over a period of several years.[24–27] For this work the surface was prepared at room temperature by several cleaving procedures. In the earliest work the samples were simply cleaved in air and then inserted into the HAS instrument. Later, the samples were cleaved *in situ* with one of two different types of cleavers. One of these employed a pair of jaws to apply pressure to a notched KCN crystal; the other used a guillotine with a spring-loaded knife that was driven against the crystal. In each case a careful search for indications of the surface structure was carried out over a range of incident wave vectors and for target temperatures spanning the cubic to antiferroelectric regimes. However, in spite of considerable effort to measure the expected specular and Bragg diffraction features by HAS [as was so easily done for KBr(001) (Ref. 2)], no peaks in the helium angular distribution, which would have provided evidence for long-range order, were ever found.[25,27] A typical angular distribution for this surface is shown in Fig. 1(b).[27] Furthermore, time-of-flight (TOF) measurements of the inelastic helium atom scattering typically yielded spectra with only a diffuse elastic peak on a broad multiphonon background, not the single annihilation and creation surface phonon peaks usually seen from ordered surfaces.[2,25] The conclusion reached through these efforts was that under the conditions of our experiments the KCN(001) surface is disordered.[24,25,27]

KCN in its rocksalt structure phase and KBr are closely matched in lattice dimensions, at 6.53 Å and 6.59 Å, respectively. In the work reported here a monolayer KCN film was grown onto a KBr(001) substrate, which pins the structure of the KCN film through strong ionic interactions. The structure and dynamics of this film, which was found to possess long-range order, could then be studied over a wide range of temperatures. Unlike the bulk material, only a single phase transition, a second-order transition to an antiferroelectric alignment of the CN^- ions at $T = 97$ K, was observed. The temperature range studied was approximately 60–300 K.[24,26,27]

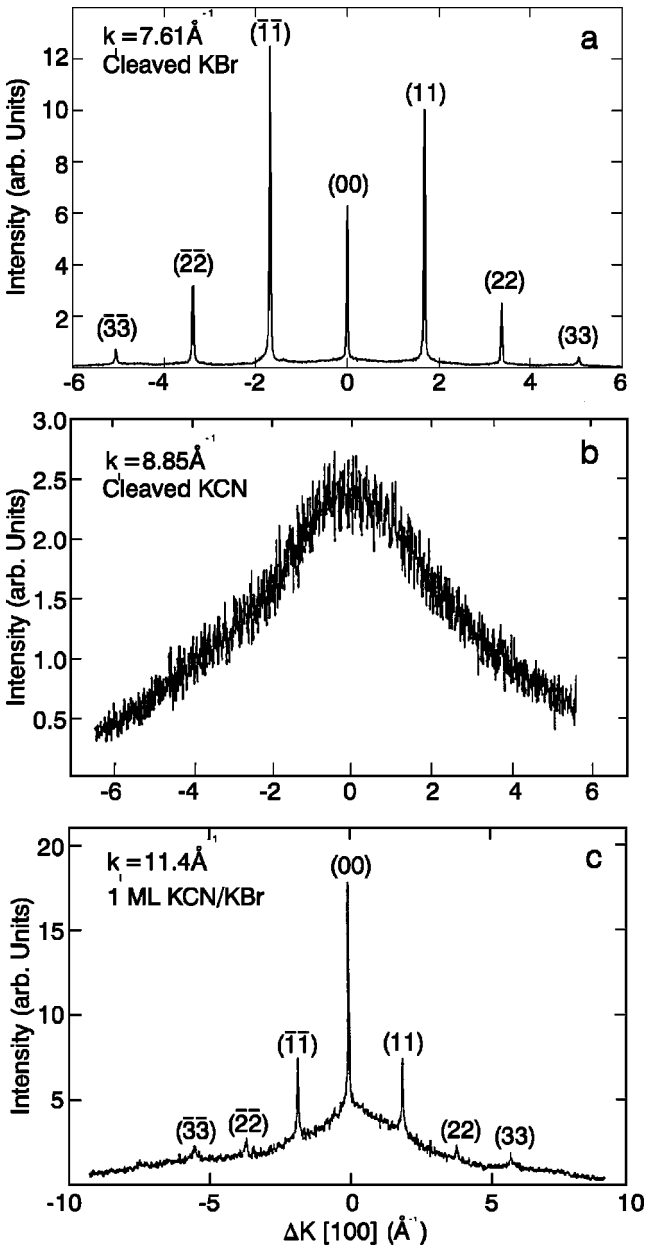

FIG. 1. (a) An angular distribution, helium scattering intensity vs parallel momentum transfer ΔK (see experimental section for definitions), from the (001) surface in the [100] azimuth of a KBr crystal cleaved in air. (b) An angular distribution from an *in situ* cleaved crystal of bulk KCN. (c) An angular distribution from a KCN monolayer film pinned to a KBr(001) substrate. The specular and Bragg peaks are clearly evident and indicate long-range order. The temperature of the target is 140 K in each panel; the incident wave vectors $\mathbf{k}_i$ are indicated in each panel. The labels over the peaks are the corresponding indices of the reciprocal-lattice vectors.

The experimental method is detailed in the next section. This is followed by sections presenting the results of the measurements and discussions of the surface structure and dynamics and, finally, by a summary of the conclusions.

II. EXPERIMENTAL METHOD

High-resolution helium atom scattering is a technique for measuring surface structure and surface phonon dynamics that works equally well with all types of crystalline materials.[1,24,26] The HAS instrument used in these experiments has been reported in the literature a number of times by this group and is similar to HAS instruments used by other groups.[2,28–30]

Three general types of measurements have been made in these experiments. First, with the chopper out of the beam path, the helium scattering intensity as a function of the incident angle θ_i (or parallel momentum transfer $\Delta K = K_f - K_i$) gives an angular distribution (AD). Example AD's are shown in Figs. 1 and 2. The coherent elastic scattering of the atoms from the ordered surface gives rise to specular and Bragg diffraction in the AD's, which can be analyzed to determine the structure of the surface.[28]

In the second type of measurement, growth behavior can be observed in real time by monitoring the specular beam intensity ($\theta_i = 45°$) vs time during deposition. Figure 3 is an example that shows the specular signal in the [510] direction vs deposition time; here the growth was stopped at approximately one monolayer. A discussion and an example showing the oscillatory behavior over many monolayers of growth for KBr on RbCl is given in the work of Safron *et al.*[31]

The third type of measurement requires inserting the chopper into the beam path to provide 11 μs pulses of atoms that scatter elastically and inelastically from the crystalline target.[2,28] Energy transfer is measured by a time-of-flight (TOF) technique. Using the requirements of energy and parallel-momentum conservation and the scattering geometry, one can convert the TOF spectra carried out over a range of incident angles and energies into a surface phonon-dispersion curve (i.e., phonon energy vs phonon momentum) for the collective surface vibrations of the material. The TOF capability makes HAS the surface analog of neutron scattering from crystals. It allows one to investigate the lattice dynamics of the surface, including modifications of the surface forces due to the presence of adlayers.[1,2,28–32]

III. STRUCTURE

A. Growth of the monolayer film

The KBr substrate was cleaved in air to obtain a (001) surface and then inserted into the vacuum chamber. After achieving pressures in the low-10^{-10} torr range, the KBr target was cleaned by flashing to 650 K. An AD from this surface is shown in Fig. 1(a). Following this, a small piece of single-crystal KCN was heated to sublime at a suitable rate for deposition onto the KBr substrate.[33] As discussed above, the deposition was tracked by monitoring the specular He beam intensity as a function of deposition time, which is shown in Fig. 3.

Figure 1(c) and the left panels of Fig. 2 show AD's at 140 K from a monolayer film produced in this manner. Although the background is larger than that obtained from the cleaved KBr(001) substrate [see Fig. 1(a)], the recovery of the specular intensity to nearly its pregrowth value and the presence of sharp diffraction peaks indicate that the film has considerable long-range order. TOF spectra taken from the film at similar sample temperatures generally have a large, broad inelastic component and weak diffuse elastic peaks, indicating that the large background is primarily due to inelastic scattering.

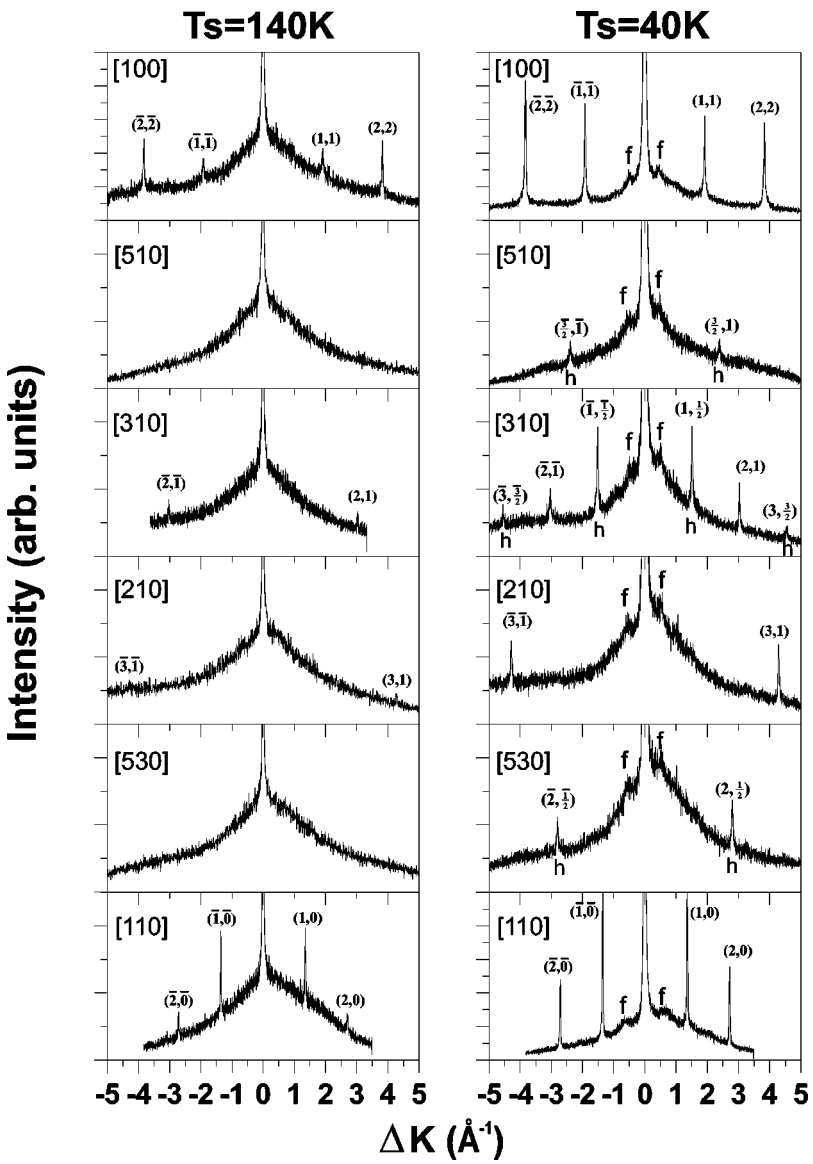

FIG. 2. A series of angular distributions, helium scattering intensity vs parallel momentum transfer, in six different azimuthal directions for target temperatures of 140 K (left panels) and 40 K (right panels) with $\mathbf{k}_i = 7.16$ Å^{-1}. The additional diffraction peaks found in the 40 K panels are labeled *h* for half-integer diffraction spots and *f* for other fractional order diffraction spots, as discussed in the text.

If the KCN growth is halted at a time corresponding to roughly a half monolayer, then a measurement of the specular intensity as a function of momentum transfer perpendicular to the surface exhibits oscillations consistent with interference from single steps, indicating that the film grows as a single atomic layer.[27]

In the left panels of Fig. 2 the integer order diffraction peaks in each of the six azimuthal orientations are labeled by the corresponding reciprocal-lattice vector indices and are consistent with the diffraction expected from a (1×1)-KCN(001) surface. Note that in the [510] and [530] directions no integer order diffraction peaks are expected except for the specular reflection, (0,0), as they all lie beyond the accessible angular range at this incident wave vector 7.16 Å^{-1}.

Attempts to continue growth of the film to a second layer and beyond were not successful. No further oscillations in the deposition curve were observed; rather, the intensity just decayed monotonically.[24] The AD's from films obtained by depositing KCN for a time that should have corresponded to a second layer only yielded a small specular reflection, but no other Bragg diffraction features. This suggests that this

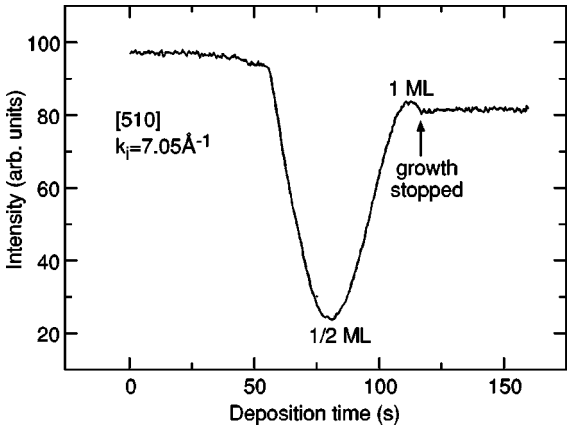

FIG. 3. The specular intensity in the [510] azimuth during the deposition of KCN onto KBr(001). The deposition starts at approximately 50 sec and is stopped at about 100 sec after a single monolayer has been deposited. If the deposition had continued for another 50 sec (equivalent to two layers of KCN), the specular intensity would have decreased monotonically. The angular distribution measured for a 3-monolayer film is similar to that observed from cleaved KCN shown in Fig. 1(b).

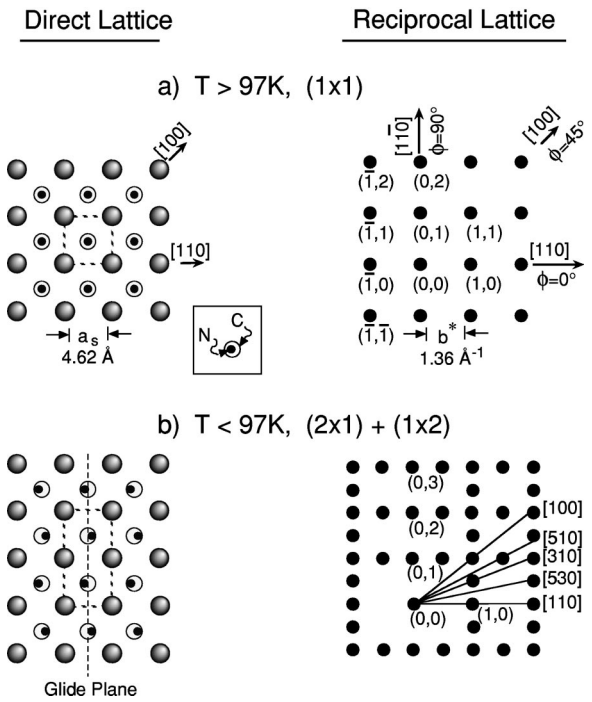

FIG. 4. Schematic representations of the direct lattice and reciprocal lattice for the two observed phases of the KCN film. The upper panel (a) depicts the (1×1) phase at temperatures above 97 K; the lower panel (b) depicts a (2×1) direct lattice and the $(1\times2)/(2\times1)$ reciprocal lattice for temperatures below 97 K. The unit cells for each direct lattice are indicated with dashed lines; in (b) the glide plane is also indicated by a dashed line.

surface is perhaps more ordered than that of the cleaved KCN crystal, which produced the data of Fig. 1(b), but much less than that of the monolayer film. After depositing for times that corresponded to 3 monolayers, the scattering from the film appeared the same as that from the cleaved KCN crystal, Fig. 1(b).[24] Our efforts reported in this paper, therefore, have concentrated on the monolayer film.

B. Phase transition

In addition to the AD's from the KCN/KBr(001) film measured at 140 K, Fig. 2 also shows AD's at 40 K at the same six azimuthal orientations. That a phase change has occurred in going from 140 K to 40 K is evident in the extra peaks in the panels on the right side that are not present in the panels on the left side of the figure.[26] The additional peaks have been labeled *h* for the half-integer diffraction orders and *f* for the other fractional orders. We defer a discussion of the latter to a later section.

Reciprocal space peak positions and corresponding real-space structures consistent with the phases above and below the transition are shown in Fig. 4. The diffraction peaks in the AD's taken at 140 K correspond to the expected reciprocal-lattice points for the (1×1) unit cell and are shown in the top half of the figure. We have pictured the CN^- ions in the (1×1) structure to be aligned (approximately) perpendicular to the plane of the surface with the N end up to conform to the results of calculations for the surface orientational distribution in KCN(001).[13] We cannot tell from our experiments what the alignment of these ions actually is, only that the surface is (1×1).

The additional peaks found at 40 K labeled *h* in Fig. 2 correspond to the reciprocal-lattice points at half-integer positions in Fig. 4. Of the measured directions, these peaks were seen in [510] and [310] azimuths. They indicate that at 40 K the structure has changed to (2×1)- and (1×2)-oriented domains. Due to the lack of evidence for a displacive transition, such as the structural changes or phonon mode softening seen in bulk KCN, the low-temperature phase almost certainly results from an antiferroelectric alignment of the CN^- ions. The missing half-order spots in the [110] direction at temperatures below the phase transition indicate a structure with a glide plane.[34] In turn, this implies that the modulated component of the CN^- orientations, which is responsible for the $(2\times1)/(1\times2)$ structure, must lie solely in the plane of the surface, perpendicular to the glide plane.

In comparing the surface phase transition found here with the transitions for KCN observed in the bulk, we point out two important differences and two similarities. First, there appears to be only one transition for the monolayer film, whereas two phase changes occur in the bulk solid phase. Second, the very large structural shifts that accompany the bulk transitions are not seen for the KCN film, apparently because of the pinning by the KBr substrate noted earlier. For both film and bulk, on the other hand, the ultimate alignment of the CN^- dipoles is antiferroelectric, and the order of the transition leading to this alignment appears to be second order (see below).

C. Order of the phase transition in pure and mixed crystals

To determine the order of the transition for the film, the temperature dependence of the intensity of the one-half order Bragg peak was measured in the [310] direction (see Fig. 2). This peak was chosen because it is an unambiguous feature of the low-temperature phase and is reasonably intense. For a second-order transition, the intensity is proportional to the square of the order parameter and is expected to follow the relation $I/I_0=[(T_c-T)/T_c]^{2\beta}$ below and near the transition temperature T_c.[35] Here I is the normalized intensity at temperature T, I_0 is the normalized intensity at $T=0$ K, and β is a critical exponent. This expression is borrowed from neutron-scattering studies where it has been used to determine T_c and β from the temperature dependence of diffraction peaks induced by second-order phase transitions, often half-integer peaks associated with antiferromagnetism.[36] This same relation has been employed in a recent HAS study of the antiferroelectric behavior of the (001) surface of $KMnF_3$.[35]

The results of the measurements are shown in Fig. 5. In this plot, the contribution to the temperature dependence of the half-order peak due to the Debye-Waller effect was approximately removed by normalizing the peak intensity to that of the specular reflection at the same temperature, as both diffraction peaks should have similar Debye-Waller factors. The intensity of the half-order Bragg peak has no discontinuous jumps and exhibits no hysteresis upon temperature cycling, consistent with a second-order transition. The analysis of the fit yields $T_c=97$ K and $\beta=0.28$.

For doped bulk crystals, $KBr_x(CN)_{1-x}$, where x is the mole fraction of the Br^- ion and $1-x$ the concentration of

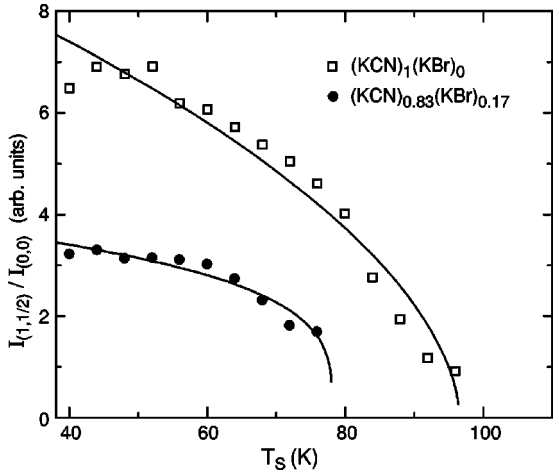

FIG. 5. The ratio of the scattering intensity of the half-order peak in the [310] azimuth to the specular intensity as a function of temperature. The open squares are taken from a monolayer of KCN on KBr(001); the solid circles are from a monolayer formed by codeposition of KBr and KCN onto KBr(001) with an approximate composition of 83% KCN and 17% KBr. The transition temperature T_c is 97 K for the KCN film and 78 K for the mixed film.

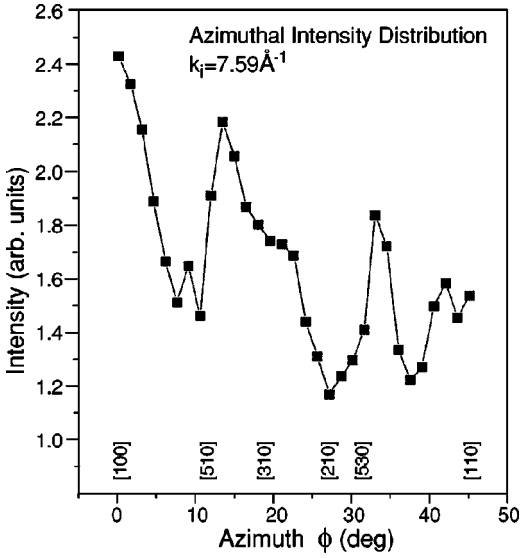

FIG. 6. A plot of the fractional order peak intensity (labeled *f* in Fig. 2) as a function of azimuthal angle. The azimuthal directions are included along the abscissa. The peaks are judged to be along [100], [310], [530], and [110]. Note that the ordinate scale does not start at zero intensity.

the CN^- ion, the transition temperature for the phase change decreases with decreasing CN^- concentration[16–23] until a sufficiently low CN^- concentration is reached where the phase change no longer takes place.[23]

In the current instrumental configuration, growing mixed $KBr_x(CN)_{1-x}$ surfaces is somewhat awkward. However, we were able to carry out one set of experiments with a film of the approximate composition $KBr_{0.17}(CN)_{0.83}$. This film was prepared on a KBr substrate by codepositing KBr and KCN. Separate KCN and KBr sublimation sources were used after the growth rates of both were determined as a function of temperature. The temperatures were then adjusted for each source, and both shutters were opened simultaneously to codeposit the film. A plot of the ratio of the half-order peak intensity to the specular intensity in the [310] direction vs substrate temperature for this film is also shown in Fig. 5. The transition temperature T_c for the mixed film is 78 K, with $\beta = 0.13$.

The results for the β's must be regarded as very preliminary because of the uncertainties and the limited amount of data near T_c, particularly for the mixed case. However, the transition temperature has clearly decreased when the CN^- ion concentration was reduced.

Further work needs to be carried out to determine the dependence of the transition temperature on the concentration *x*. We expect that theoretical modeling of the phase transitions in these mixed ultrathin films will prove to be both simpler and more revealing than has been achieved with models for the bulk phase transitions.

D. $2\sqrt{2}\times 6\sqrt{2}R45°$ structure

The fractional-order diffraction peaks labeled *f* in Fig. 2 are much smaller and broader than the half-integer diffraction peaks, but appear at the same transition temperature. They range in position from $\Delta K = G_{1,1}/4$ in the [100] direction to $G_{1,0}/2$ in the [110] direction. (Note that we have labeled this half-order peak in the [110] azimuth as an *f* peak rather than an *h* peak because of its characteristic appearance.) Since $G_{1,1} = \sqrt{2}G_{1,0}$, the momentum transfer increases with azimuthal angle ϕ going from 0° to 45° (corresponding to the orientations [100] and [110], respectively).

To understand this behavior better, a careful search of the azimuthal dependence of the intensities of these peaks was made to determine what surface structure they might represent. The measurements were carried out at azimuth intervals of 1.5° that, because of weak intensities, nearness to the specular peak and limited azimuthal angular positioning capability ($\pm 0.15°$), produced the somewhat scattered data of Fig. 6. The measurements were repeated twice with similar results. Four broad, overlapping intensity maxima were determined between $\phi = 0°$ and 45°, which we have provisionally associated with reciprocal-lattice points lying in the directions [100], [310], [530], and [110]. The simplest direct lattice that gives diffraction peaks consistent with this assignment is the $(2\sqrt{2}\times 6\sqrt{2})R45°$ structure shown schematically in Fig. 7. That is, there must be a corrugation in the surface electronic density corresponding to this structure to give these diffraction peaks in the helium scattering, in addition to that which is responsible for the $(1\times 2)/(2\times 1)$ diffraction features, if our assignment is correct. Because of the fourfold symmetry of the original (1×1) surface, we would expect the surface to have domains with both this structure and a similar structure rotated by 90°. Since the peaks are very broad, the implication is that these domains are not very large and not uniform in size. Additional experiments and, particularly, theoretical work need to be done to understand the full implications of the diffraction studies.

E. Surface Debye temperature

The Debye-Waller expression can be written in the approximate functional form $I = I_0 \exp(-a|\mathbf{k}|^2 T)$ where $\mathbf{k} = \mathbf{k}_f$

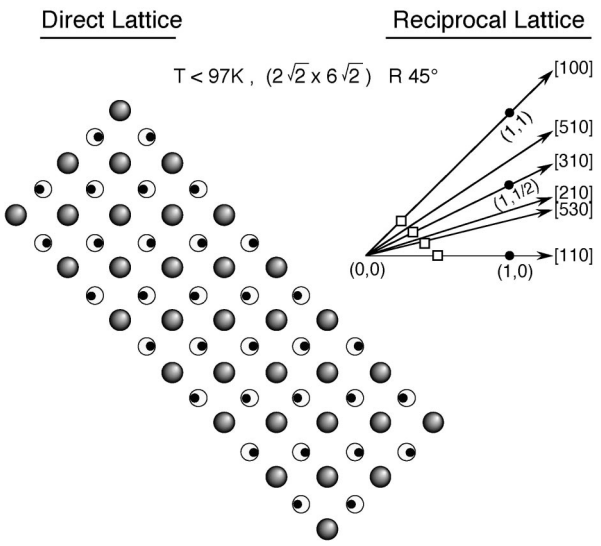

FIG. 7. The reciprocal-lattice points corresponding to the broad peaks from Fig. 6 (right), and a schematic depiction of the $(2\sqrt{2} \times 6\sqrt{2})R45°$ direct-space lattice consistent with those peaks (left).

$-\mathbf{k}_i$ is the momentum transfer and $a = 3\hbar^2/(Mk_B\Theta_s^2)$, with Θ_s the surface Debye temperature, M the mass of the vibrating atoms in the surface, k_B the Boltzmann constant, and I and I_0 the scattering intensities at temperatures T and $T=0$ K, respectively.[25,37] A fit to the helium specular reflection intensities for a monolayer film of KCN/KBr(001) at $k_i = 7.68$ Å^{-1} over a range of temperatures gave $a = 1.2 \times 10^{-5}$ Å^2 K^{-1}. No difference was noticed in the value of a above and below the transition temperature. There is some uncertainty in this approximation in how one should choose the value for M when there is more than one atom per unit cell. However, a reasonable choice is to take $M = M_K + M_C + M_N$, which gives $\Theta_s = 136$ K, close to the value of 123 K obtained in a HAS study of the multiphonon scattering from the cleaved surface of KCN.[25] When the same measurements are made on a clean KBr(001) surface, one finds that the quantity $a = 1.1 \times 10^{-5}$ Å^2 K^{-1}, which is nearly the same as for the monolayer KCN film. However, M for KBr is somewhat larger, and one obtains $\Theta_s = 105$ K. For comparison, the bulk Debye temperature for KBr is $\Theta_D = 173$ K;[38] the surface Debye temperature should be approximately two-thirds of this or 115 K, which is close to the measured value.

IV. DYNAMICS

The primary source of data regarding the lattice dynamics of crystalline materials has been from inelastic neutron-scattering measurements. However, perhaps because of the large Debye-Waller factors and multiphonon scattering,[8] the extent of such data for the alkali cyanides is relatively meager.[7,8,24,39] For KCN, enough data have been obtained to construct the dispersion curves for the acoustic modes, but only very few points exist for the optical modes. Hence, the dynamics of this material is not as well understood as, for example, the alkali halides. HAS experiments to determine the surface phonon dispersion can therefore make a significant contribution to our understanding of these dielectric materials. This scarcity of data from bulk studies was one motivating factor for the present surface dynamical measurements. A second factor is that with the additional freedom of the CN^- rotations or librations, KCN ought to exhibit different surface mode behavior than that observed for the alkali halides.

The TOF method was used to measure the surface phonon dispersion of the (1×1)-KCN monolayer film in the [100] and [110] high-symmetry directions of the surface Brillouin zone. Measurements were also made in these same directions at temperatures below the transition to the $(1\times2)/(2\times1)$ phase. In carrying out the TOF experiments, it was observed that the signals degraded over a period of a couple of hours when the sample temperatures were below approximately 130 K. For the low-temperature studies, then, the data collection was periodically halted (approximately hourly) in order to flash the target to 325 K for cleaning. For measurements at 140 K and above, this procedure proved to be unnecessary. The film did not appear to be otherwise affected by this heating. About 300 individual TOF spectra were accumulated in all.

The single phonon creation and annihilation peaks in the TOF spectra were transformed into phonon energy and phonon wave vector in the usual way.[1] The points obtained for the film in both the (1×1) and $(1\times2)/(2\times1)$ phases in the [100] high-symmetry direction are shown in an extended zone plot in the upper panel of Fig. 8. The points shown as solid squares are from TOF peaks that can be analyzed with the greatest certainty, whereas the ones represented by open squares correspond to peaks in the spectra that are less well defined and have somewhat more uncertainty. Since the helium atoms interact most strongly with the sagittal plane vibrational modes that have significant polarization normal to the surface, the points in the diagram probably represent those film modes most polarized in this way.[1]

In the lower panel of Fig. 8, the ''best'' points from the upper panel are shown in a reduced zone plot as the open circles for the high-temperature phase data and as the solid circles for the low-temperature phase data. Also in this figure are the more limited number of data points from the high-and low-temperature phases measured in the [110] azimuth. Nearly all the data in the figure were taken at 40K for the $(1\times2)/(2\times1)$ phase and at 140 K for the (1×1) phase. Finally, the large, numbered open squares placed at the zone center and zone boundary lines mark points of comparison of the phonon energies of the film with the corresponding phonons of the KBr substrate surface and with those of the KCN bulk.

The points in the lower panel of Fig. 8 seem to fall into three groups: The Rayleigh wave (or lowest-energy surface phonon dispersion branch), which rises from 0 meV at the zone center to near 5 meV at the zone boundaries; a very flat optical mode at about 11.5 meV; and several isolated points, including three at high energy $\sim$18 meV, one low-energy point ($\sim$2 meV) in the middle of the $\bar{\Gamma}$-$\bar{M}$ region of the surface Brillouin zone, and another near $\bar{X}$, and two medium-energy points at about 9 meV. The phonon energies measured above and below the transition temperature essentially lie on the same curves. Further, whereas the transverse

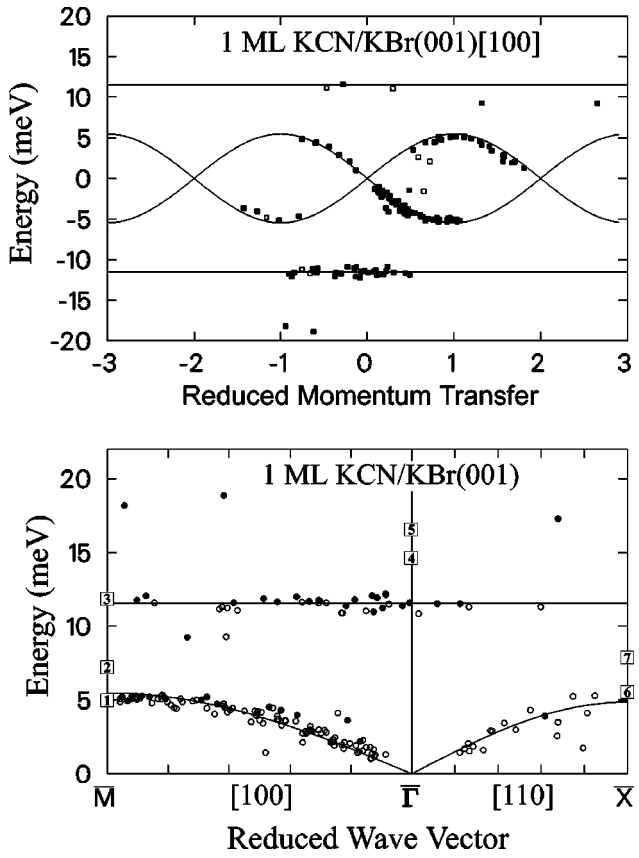

FIG. 8. An extended Brillouin-zone plot of the surface dispersion data for the monolayer KCN film in the [100] high-symmetry direction (upper panel) and a reduced zone plot of the data in both [100] and [110] high-symmetry directions (lower panel). The ''best'' points in the upper panel, as described in the text, are shown by solid squares while the data of slightly lower quality are shown as open squares. Only the best points in the upper panel (solid points) are plotted in the lower panel, where the open circles are from data taken with the film in the high-temperature phase and the solid circles are from the film in the low-temperature phase (see text). The thin solid lines at about 11 meV and the sinusoidal curves in both panels have been drawn through some of the data (as discussed in the text) to guide the eye. The numbered squares in the lower panel are points of comparison with phonon energies of the substrate KBr(001) and of bulk KCN: 1, 5.2 meV for the KBr(001) at $\bar{M}$; 2, 7.5 meV for the bulk KCN [100] zone boundary; 3, 12.2 meV for the KBr(001) S_2 mode at $\bar{M}$; 4, 14.8 meV average for the bulk KCN libration (Ref. 6); 5, 17 meV for the bulk KCN TO mode [model (Ref. 39)]; 6, 5.6 meV for the KBr(001) at $\bar{X}$; 7, 7.9 meV for the bulk KCN [110] zone boundary. The abscissa scale in the lower panel is in units of the surface Brillouin zone: at $\bar{X}$ the value is 0.68 $Å^{-1}$ and at $\bar{M}$ 0.96 $Å^{-1}$. In the upper panel the abscissa units are the same as the value at $\bar{M}$.

acoustic dispersion branch for the KCN bulk phonons had an unusual ''s'' shape with an upward curvature near the zone center,[7,8,10,39] the Rayleigh wave appears more typically linear for small values of the reduced wave vector.

A striking feature of the dispersion curves is that there is no evidence of the mode softening that occurs in the bulk because of the phase transition.[10] One could speculate that the reason mode softening is not observed is that the forces responsible for the antiferroelectric ordering of the CN^- ions primarily affect modes that are polarized in the surface plane and do not interact strongly with the impinging helium atoms. However, especially with the absence of evidence in the elastic scattering for the kind of structural changes seen in the bulk, it is more likely that the phase transition does not involve the softening of a phonon mode into a static displacement but rather is an order-disorder transition to the antiferroelectric alignment. Like the stability of the film itself, the lack of a displacive transition may be a result of the strong ionic interactions with the substrate.

In both the [100] and [110] directions, the Rayleigh wave of the film resembles the Rayleigh wave of the substrate KBr.[2] The energies at $\bar{M}$ and $\bar{X}$ are nearly the same and their shapes are similarly gently curving. (The sine curves in the lower panel of Fig. 8 have been drawn to guide the eye.) A minor deviation is that the dispersion curve for the film mode seems slightly higher than that for the substrate in the [100] azimuth but slightly lower in the [110] azimuth. More significant is the comparison with the corresponding bulk transverse-acoustic (TA) mode energies. At the zone boundary in the [100] direction, the bulk KBr TA mode has an energy of about 5.2 meV,[40] very nearly the same as for the film and for the KBr(001) surface, whereas that for KCN is 7.5 meV.[39] One expects that at the zone boundary the mode energies should scale as the inverse square root of the ratio of the heavier masses if the interactions are approximately equal.[1] As the heavier mass in the substrate is approximately equal to 80 for Br, and in the film 39 for K, the ratio of energies for KCN to KBr ought to be about 1.4. This is about right for the bulk energies, but clearly way off for the film. (This assumes that the CN^- ion with its very strong triple bond between the C and N acts as a single particle.) In the [110] direction the situation is very much the same.

In the inelastic helium scattering experiments on cleaved KBr(001) (Ref. 2) a ''crossing mode'' was found in both high-symmetry directions that had intensities comparable to those measured for its Rayleigh phonons. This mode has its origin in the bulk transverse-acoustic branch, but it has optical character as a surface vibration. There is no evidence at all of this dispersion branch in these experiments for the KCN film. Thus, one explanation for the similarities of the KCN film and KBr substrate Rayleigh waves is that the reduced coordination of the KCN at the surface has lowered the vibrational energies across the Brillouin zone, coincidentally, nearly to those of the substrate phonons. Another is that the acoustic-mode-like displacement pattern of the substrate Rayleigh wave dominates the vibrations of the ultrathin film so as to reflect the vibrational characteristics of the KBr rather than of the KCN.

The flat mode in both symmetry directions at 11.5 meV is curious for several reasons. First, the intensity of the scattering for these optical modes in these experiments was generally strong, particularly in the [100] azimuth, whereas very few optical mode data points were observed in neutron-scattering studies.[7,8,39] Second, the energy of this mode is close to but distinctly below those measured for the S_2 surface band-gap mode of KBr (Ref. 2) and well below that for the calculated optical mode of bulk KCN.[39] It is also much flatter than these modes. Third, as with the acoustic branch, the optical modes should scale with mass at the zone bound-

ary and also at the zone center.[1] At $\bar{M}$ the factor should be approximately the inverse square root of the lighter masses, K for KBr and CN for KCN, or $\sqrt{26/39}=0.82$. At $\bar{\Gamma}$ the factor goes as the inverse square root of the reduced masses, or $\sqrt{15.6/26.2}=0.77$. Hence, as for the Rayleigh wave, this surface branch does not appear to scale properly with mass. The flatness of the branch suggests that the motion within each unit cell associated with this vibration is essentially uncoupled from that in all the other unit cells, i.e., the modes are Einstein-like. This suggests a more interesting and more speculative explanation for the origin of the 11.5-meV flat mode, namely, that it arises from librational motions of the CN^- ions. A librational mode has been measured in the bulk through Raman scattering, which has energies that range from 14 to 15.6 meV as the temperature is lowered from about 150 K to 50 K.[6–8] The reduced coordination for these ions at the surface could account for the slightly lower energy. However, arguing against this speculation is the absence of any temperature dependence for this mode in the film.

The three high-energy points at around 18 meV lie above any seen in the experiments that were carried out on KBr(001). The high-energy modes have nearly the same energy as, and might be related to the single longitudinal-optical high-energy phonon that was measured with neutron scattering in bulk KCN studies by Rowe *et al.*[8] However, without detailed model calculations of the surface lattice dynamics, it is difficult to make any assignments at this time.

The two points that lie beneath the Rayleigh wave (one in each azimuth) and the two medium-energy points (around 9 meV) are not well understood at this time.

V. CONCLUSIONS

Helium diffraction experiments were carried out that show that an ordered monolayer film of KCN has been grown onto the substrate KBr (001) which has lattice parameters that match the KCN to $<1\%$. The experiments reveal the film to exist in two phases: a high-temperature (1×1) phase that corresponds to the rocksalt structure phase of bulk KCN and a low-temperature phase that consists of ordered (1×2) and (2×1) domains in which the CN^- ions are aligned antiferroelectrically, with the modulated component of their orientations in the surface plane. The phase transition appears to be second order and occurs at $T_c\approx97$ K. The interactions responsible for this transition, therefore, are likely to be similar to those causing the second-order transition to the antiferroelectric phase in bulk KCN although that transition takes place at the somewhat lower temperature of 83 K.[11] For the film, it would appear that the K^+ ions are pinned by strong ionic forces to the substrate so that the structure of the low-temperature phase remains commensurate instead of undergoing large distortions from cubic as it does in the bulk. In addition to the strong and sharp diffraction spots related to the $(1\times2)/(2\times1)$ structure in the low-temperature phase, weak broad spots are also observed near the specular reflection (small ΔK's) that suggest an additional corrugation in this phase. This diffraction suggests a larger scale arrangement that has been provisionally described as $(2\sqrt{2}\times6\sqrt{2})R45°$. The significance of this corrugation is not yet understood.

The TOF measurements of the dispersion curve in the [100] and [110] high-symmetry directions show clear evidence for a Rayleigh wave and a very flat, optical-like higher-energy (~11.5 meV) branch. The former appears very similar in shape and energy to the Rayleigh wave of the KBr substrate; the latter is slightly lower in energy and much flatter than the optical S_2 band-gap mode found for KBr(001). No evidence of mode softening or of other differences in these dispersion branches was observed in experiments carried out at target temperatures above and below the transition temperature. However, a few phonon modes were found at much higher energies (near 18 meV) for the film in the low-temperature phase and two were measured at energies below the Rayleigh wave for the film in the high-temperature phase. Two additional phonons were observed, one in each phase, at medium energies (~9 meV).

Several significant structural and dynamical issues have been raised by the measured behavior of this monolayer film that have implications for the understanding of the thin-film properties of dielectric materials like KCN. These include the nature of the antiferroelectric phase transition and the role the substrate plays in it, the identification of the phonons (if any) involved in the phase transition, the connection between librational motions and other lattice vibrations, the coupling between substrate and film vibrational modes, and the origin of interface modes, among others. To resolve these issues requires model calculations. For example, the formalism of Zieliński and Michel[13] could be applied to the structures of the monolayer film and the shell-model approach by Gillman *et al.*[32] should be suitable for the dynamics. We hope this paper might encourage such an effort.

Models of crystalline structure and dynamics can be more rigorously tested at surfaces than in studies of the bulk because the reduced symmetry of the surface does not facilitate cancellation of effects.[41] Thus, the technique employed here of stabilization via epitaxy onto a suitable substrate of an otherwise disordered surface appears to offer considerable promise as a practical method for future investigations of atomic interactions in materials.

ACKNOWLEDGMENTS

We wish to thank Professor Fritz Lüty for his generosity with samples, the Supercomputer Computations Research Institute (SCRI) of the Florida State University for computational support, and NATO Grant No. GRG. 961145 and DOE Grant No. DE-FG02-97ER45635 for financial support. We further thank Professor J. P. Toennies and the Max-Planck-Institut für Strömungsforschung, Göttingen, for their hospitality during the time when some of the analysis part of this work was performed.

[1] S. A. Safron, Adv. Chem. Phys. **95**, 129 (1996).
[2] G. Chern, J. G. Skofronick, W. P. Brug, and S. A. Safron, Phys. Rev. B **39**, 12 828 (1989).
[3] W. D. Seward and V. Narayanamurti, Phys. Rev. **148**, 463 (1966).
[4] D. L. Price, J. M. Rowe, J. J. Rush, E. Prince, D. G. Hinks, and S. Susman, J. Chem. Phys. **7**, 3697 (1972).
[5] S. Haussühl, Solid State Commun. **13**, 147 (1973).
[6] W. Dultz, Solid State Commun. **15**, 595 (1974).
[7] C. J. Bill, H. Jex, and M. Müllner, Phys. Lett. **56A**, 320 (1976).
[8] J. M. Rowe, J. J. Rush, N. Vagelatos, D. L. Price, D. G. Hinks, and S. Susman, J. Chem. Phys. **62**, 4551 (1975).
[9] K. H. Michel and J. Naudts, J. Chem. Phys. **68**, 216 (1978).
[10] J. M. Rowe, J. J. Rush, N. J. Chesser, K. H. Michel, and J. Naudts, Phys. Rev. Lett. **40**, 455 (1978).
[11] D. Durand, L. C. S. doCarmo, A. Anderson, and F. Lüty, Phys. Rev. B **22**, 4005 (1980).
[12] B. De Raedt, K. Binder, and K. H. Michel, J. Chem. Phys. **75**, 2977 (1981).
[13] P. Zieliński and K. H. Michel, Phys. Rev. B **46**, 4806 (1992).
[14] S. D. Mahanti and D. Sahu, Phys. Rev. Lett. **48**, 936 (1982).
[15] J. M. Rowe, D. G. Hinks, D. L. Price, S. Susman, and J. J. Rush, J. Chem. Phys. **58**, 2039 (1973).
[16] J. M. Rowe, J. J. Rush, N. J. Chesser, D. L. Hinks, and S. Susman, J. Chem. Phys. **68**, 4320 (1978).
[17] S. K. Satija and C. H. Wang, Solid State Commun. **28**, 617 (1978).
[18] K. H. Michel, J. Naudts, and B. DeRaedt, Phys. Rev. B **18**, 648 (1978).
[19] J. M. Rowe, J. J. Rush, D. G. Hinks, and S. Susman, Phys. Rev. Lett. **43**, 1158 (1979).
[20] K. H. Michel and J. M. Rowe, Phys. Rev. B **22**, 1417 (1980).
[21] K. Walasek and K. Lukierska-Walasek, Phys. Rev. B **48**, 12 550 (1993).
[22] F. Lüty, in *Defects in Insulating Crystals*, edited by V. M. Turkevich and K. K. Shvarts (Springer-Verlag, Berlin, 1981).
[23] J. M. Rowe, J. Bouillot, J. J. Rush, and F. Lüty, Physica B & C **136**, 498 (1986).
[24] Jeff Baker, J. J. Hernández, Jaime Li, J. G. Skofronick, S. A. Safron, and E. S. Gillman, Surf. Sci. **357-358**, 639 (1996).
[25] Srilal M. Weera, J. R. Manson, Jeff Baker, E. S. Gillman, J. J. Hernández, G. G. Bishop, S. A. Safron, and J. G. Skofronick, Phys. Rev. B **52**, 14 185 (1995).
[26] S. A. Safron, J. R. Baker, J. A. Li, E. A. Akhadov, T. W. Trelenberg, and J. G. Skofronick, in *Structure and Evolution of Surfaces*, edited by R. C. Cammarata, E.H. Chason, T. L. Einstein, and E. D. Williams, MRS Symposia Proceedings No. 440 (Materials Research Society, Pittsburgh, 1997), p. 353.
[27] Jeff Baker, Ph.D. thesis, Florida State University, 1996.
[28] G. Brusdeylins, R. B. Doak, and J. P. Toennies, Phys. Rev. B **27**, 3662 (1983).
[29] R. B. Doak, in *Atomic and Molecular Beam Methods*, edited by G. Scoles (Oxford University Press, New York, 1992), Vol. 2.
[30] R. Vollmer, Ph.D. thesis, Max-Planck-Institut für Strömungsforschung, 1992.
[31] S. A. Safron, J. Duan, G. G. Bishop, E. S. Gillman, and J. G. Skofronick, J. Phys. Chem. **97**, 1749 (1993).
[32] E. S. Gillman, Jeff Baker, J. J. Hernández, G. G. Bishop, Jaime Li, S. A. Safron, J. G. Skofronick, D. Bonart, and U. Schröder, Phys. Rev. B **53**, 13 891 (1996).
[33] Samples obtained from Crystal Growth Laboratory, Department of Physics, University of Utah, Salt Lake City, UT 84112.
[34] G. Burns and A. M. Glazer, *Space Groups for Solid State Scientists* (Academic Press, New York, 1978).
[35] J. P. Toennies and R. Vollmer, Phys. Rev. B **44**, 9833 (1991).
[36] M. Hagen, H. R. Chile, J. A. Fernandez-Baca, and J. L. Zarestky, J. Phys.: Condens. Matter **4**, 8879 (1992).
[37] *Thermal Vibrations in Crystallography*, edited by B. T. M. Willis and A. W. Prior (Cambridge University Press, London, 1975).
[38] J. T. Lewis, A. Lehoczky, and C. V. Briscoe, Phys. Rev. **161**, 877 (1967).
[39] D. Strauch, U. Schröder, and W. Bauernfeind, Solid State Commun. **30**, 559 (1979).
[40] H. Bilz and W. Kress, *Phonon Dispersion Relations in Insulators* (Springer, New York, 1979).
[41] W. Kress, F. W. De Wette, A. D. Kulkarni, and U. Schröder, Phys. Rev. B **35**, 5783 (1987).